Supporting Information

Hemiaminal-Ether Structure Stabilized by Lanthanide Complex with an Imidazole-Based Schiff-Base Ligand

Chihiro Kachi-Terajima,*[a,b] Takeru Shimoyama,[a] Takahiro Ishigami,[a] Mari Ikeda,[c] and Yoichi Habata[a,b]

[a] Department of Chemistry, Faculty of Science, Toho University, Miyama, Funabashi, Chiba 274-8510, Japan

[b] Research Centre for Materials with Integrated Properties, Toho University, 2-2-1 Miyama, Funabashi, Chiba 274-8510, Japan.

[c] Education Centre, Faculty of Engineering, Chiba Institute of Technology, 2-1-1 Shibazono, Narashino, Chiba 275-0023, Japan

*Prof. Dr. C. Kachi-Terajima

E-mail: chihiro.kachi@chem.sci.toho-u.ac.jp

Index

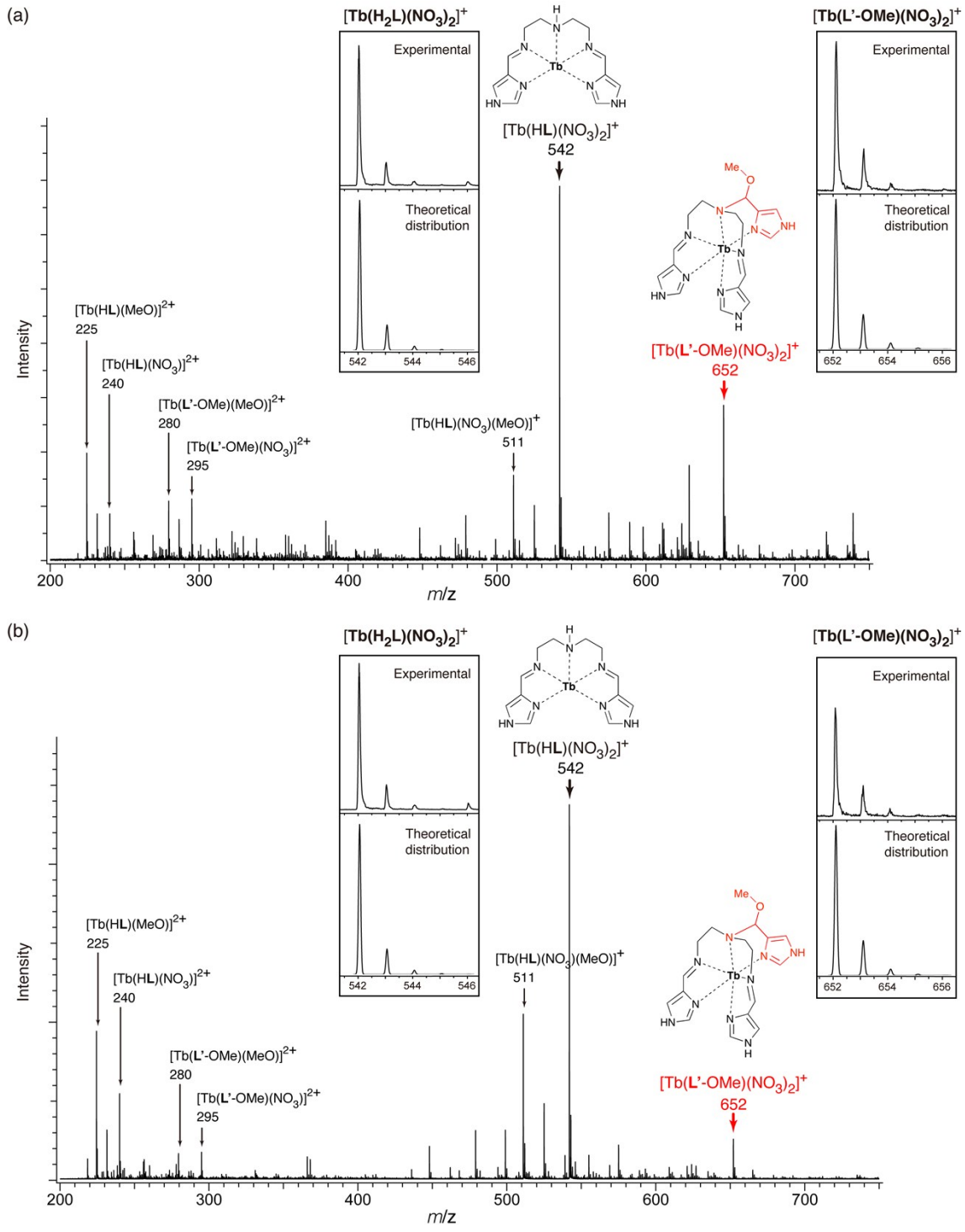

Fig. S1 CSI-MS of (a) reaction mixture of TbH**L** and 4-imidazole carbaldehyde (1 equiv.) in MeOH, and (b) methanol solution of Tb**L'**-OEt (sample concentrations, 1.0×10^{-4} M). Inset shows experimental and theoretical distribution patterns.

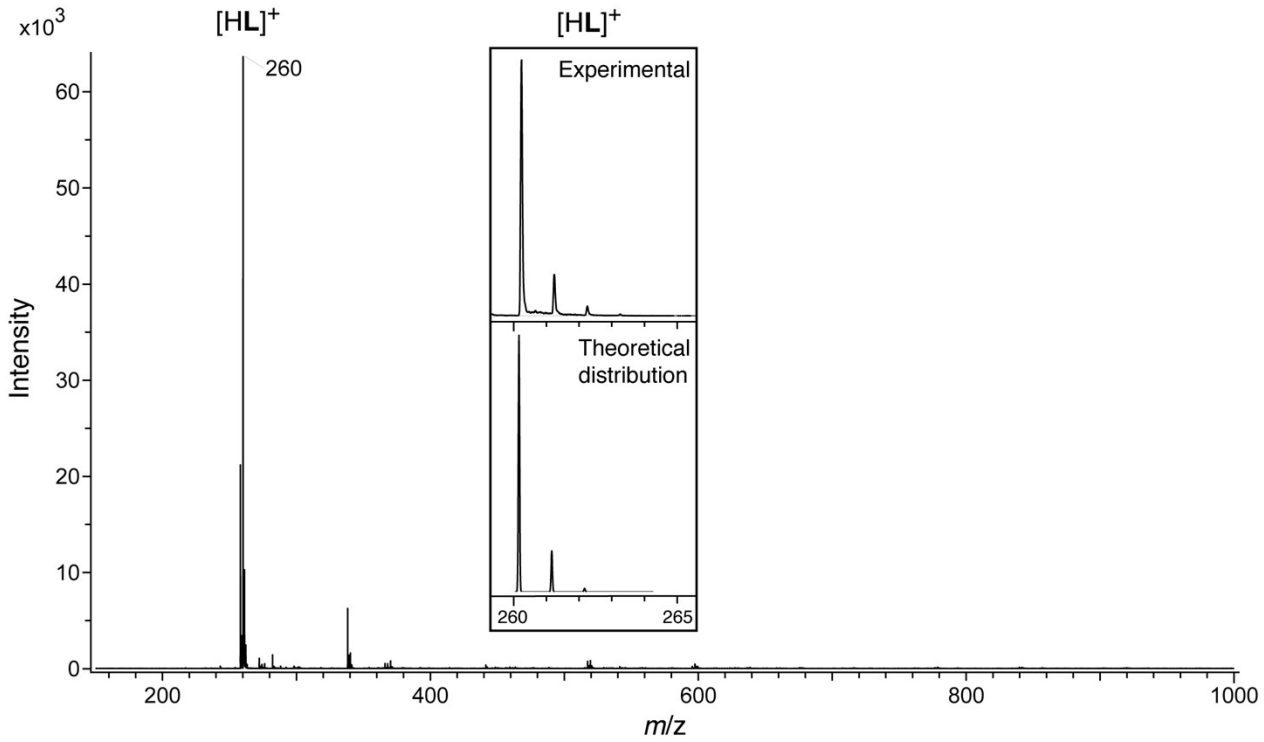

Fig. S2 CSI-MS of reaction mixture (1.0×10^{-4} M) of H**L** ligand and HNO_3 in methanol at 298 K. Inset shows experimental and theoretical distribution patterns.

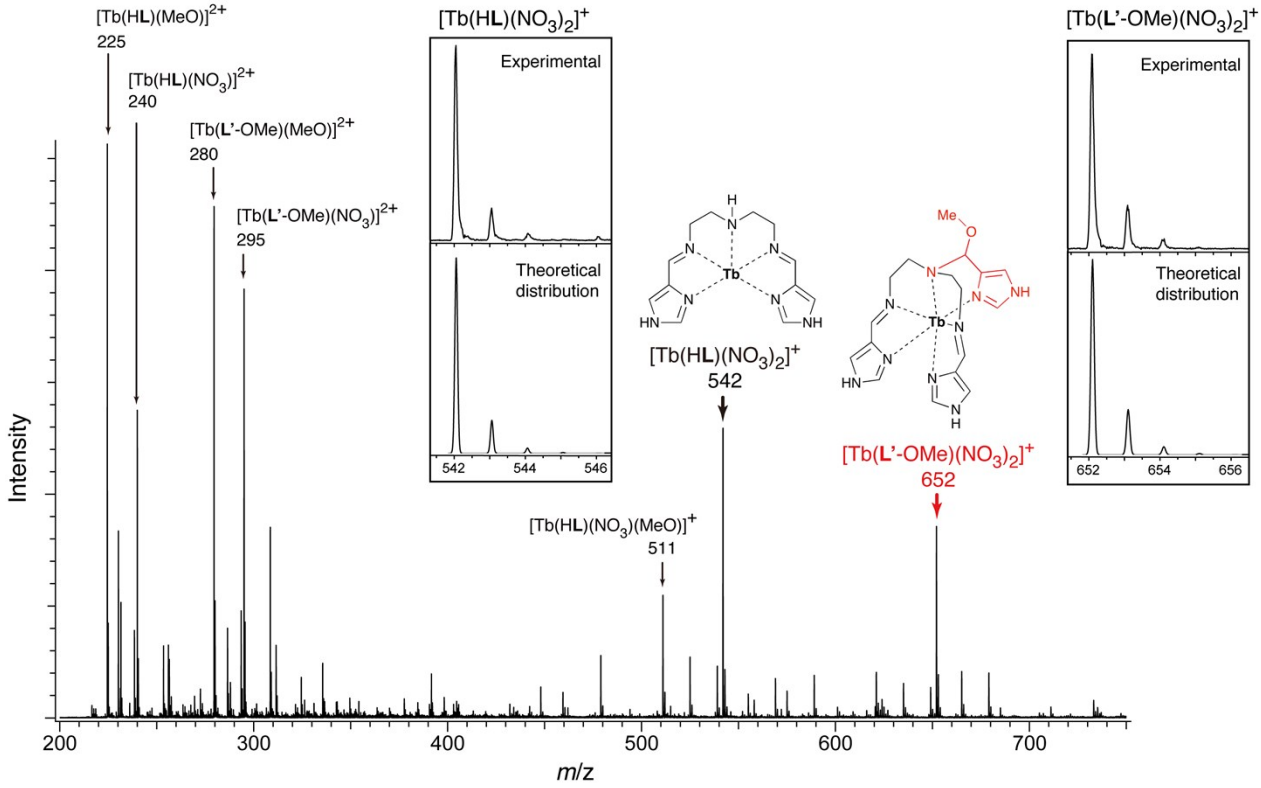

Fig. S3 CSI-MS of methanol solution (1.0×10^{-4} M) of white precipitate obtained from the reaction of TbH**L** and NO at 298 K. Inset shows experimental and theoretical distribution patterns.

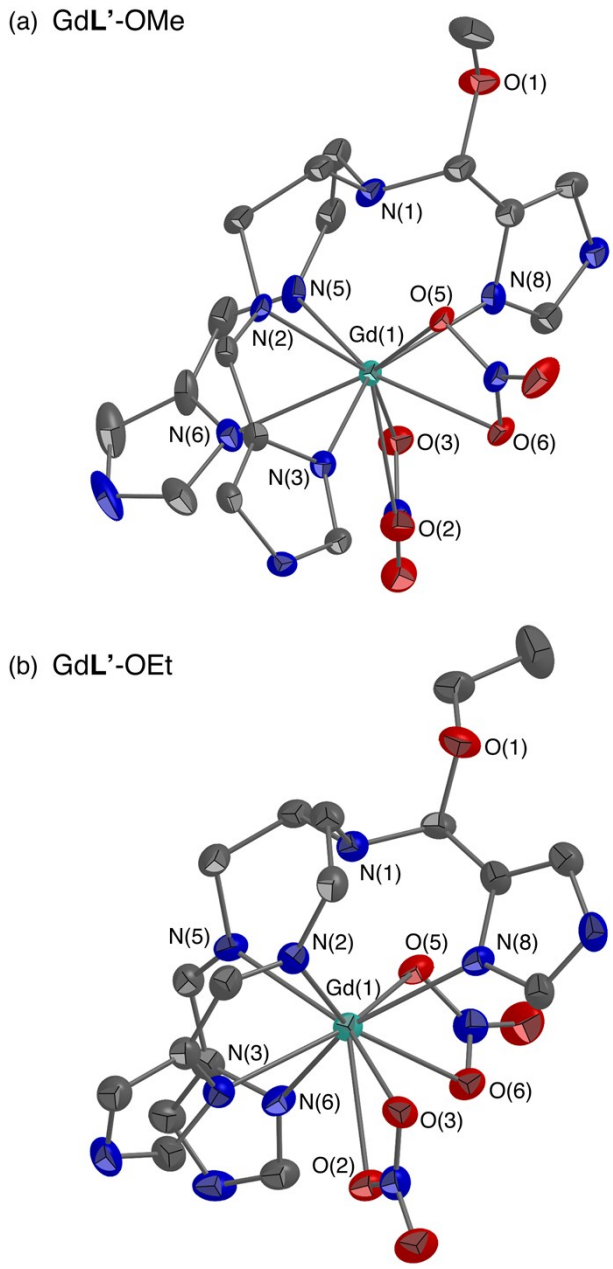

Fig. S4 ORTEP drawings of the cationic part of Gd complexes with hemiaminal-ether pendants: (a) [Gd(**L'**-OMe)$(NO_3)_2$](NO_3)·MeOH and (b) [Gd(**L'**-OEt)$(NO_3)_2$](NO_3)·EtOH. Hydrogen atoms are omitted for clarity (50% probability thermal ellipsoids).

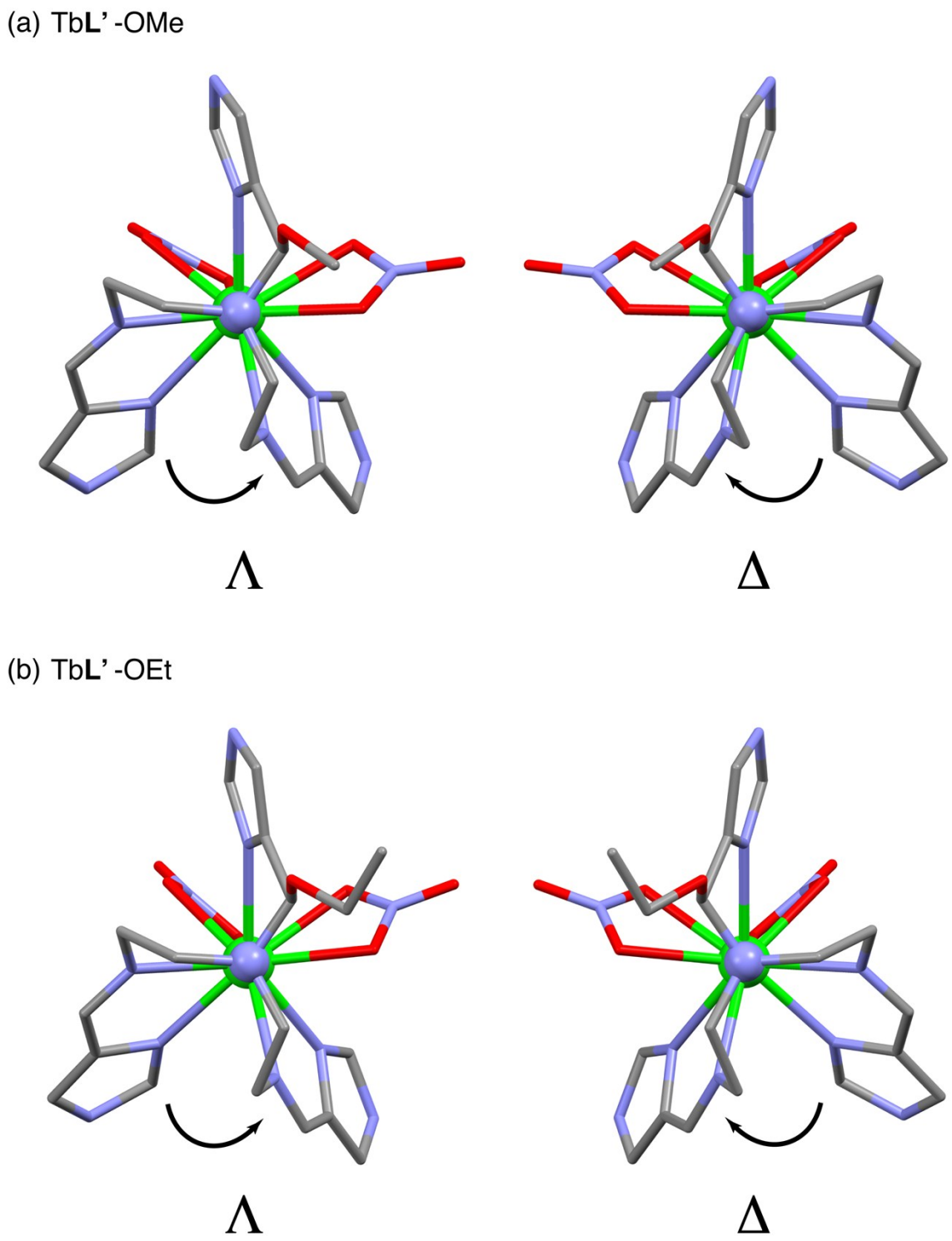

Fig. S5 Clockwise (*Δ*) and anti-clockwise (*Λ*) enantiomorphs of (a) Tb**L'**-OMe and (b) Tb**L'**-OEt.

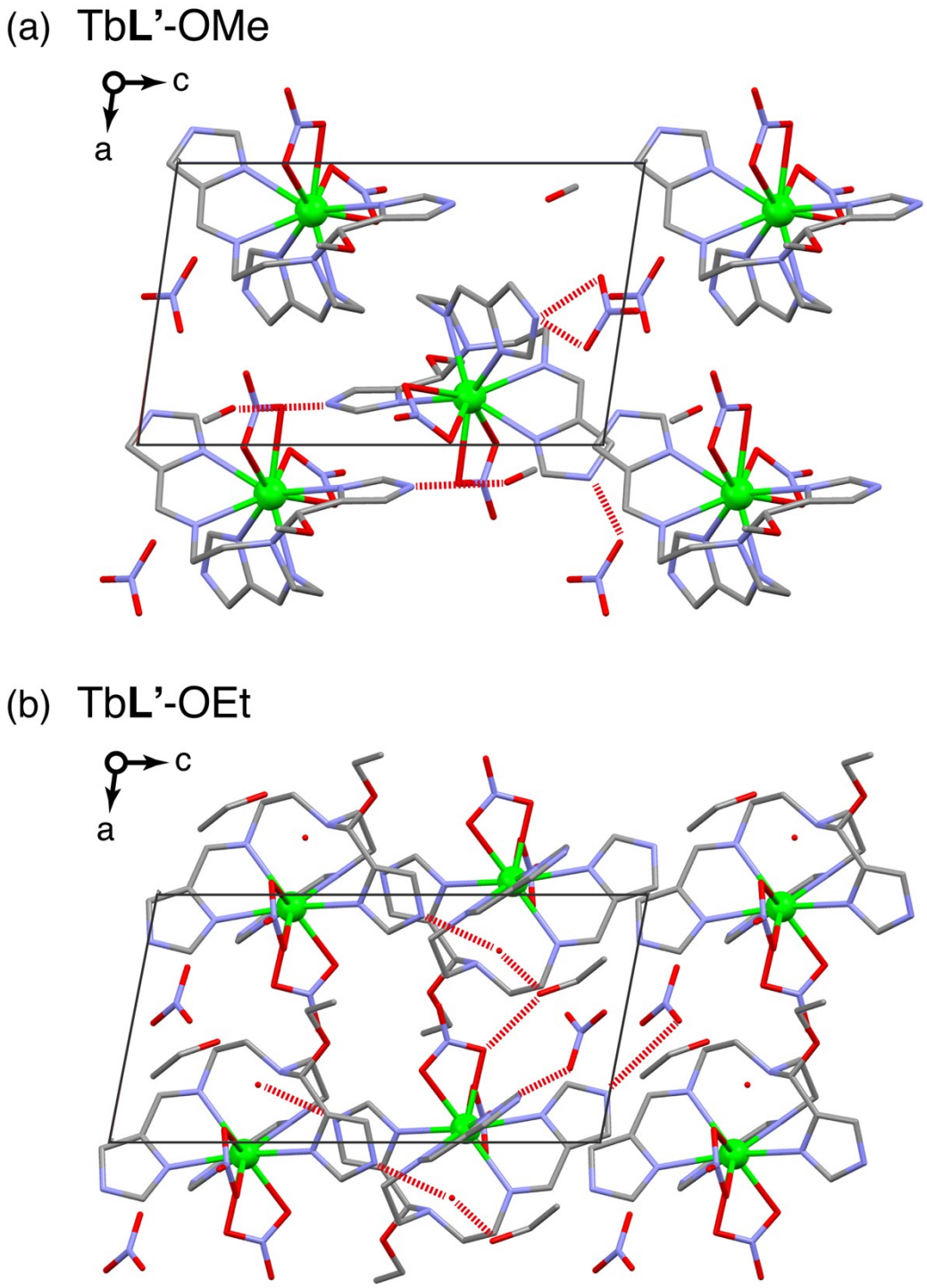

Fig. S6 Crystal packing diagram projected along the *b*-axis of (a) Tb**L'**-OMe and (b) Tb**L'**-OEt. Hydrogen atoms are omitted for clarity. Tb, N, O, and C atoms are yellow-green, purple, red, and gray, respectively. Hydrogen bonds are shown as red dotted lines.

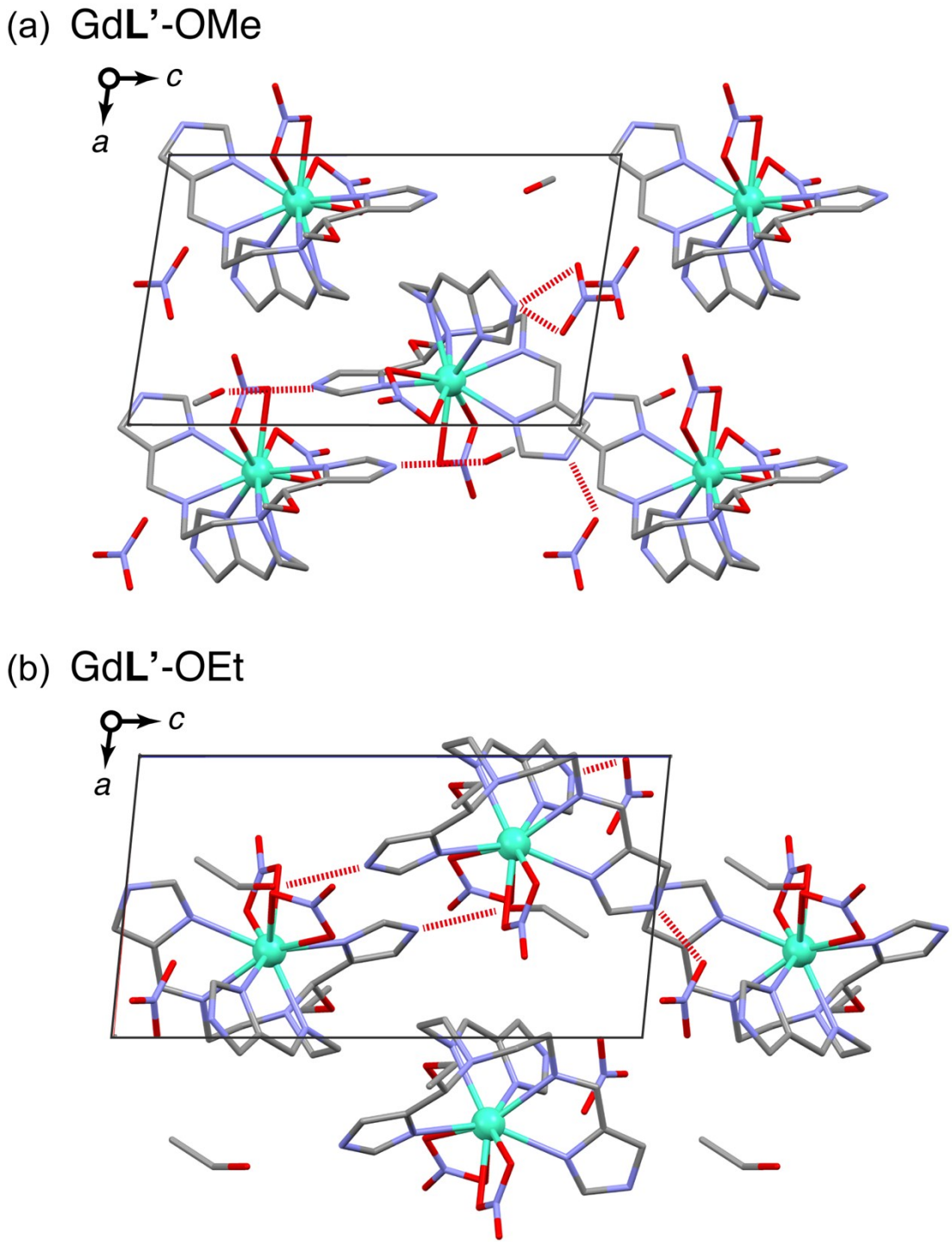

Fig. S7 Crystal packing diagram projected along the *b*-axis of (a) Gd**L'**-OMe and (b) Gd**L'**-OEt. Hydrogen atoms are omitted for clarity. Gd, N, O, and C atoms are blue-green, purple, red, and gray, respectively. Hydrogen bonds are shown as red dotted lines.

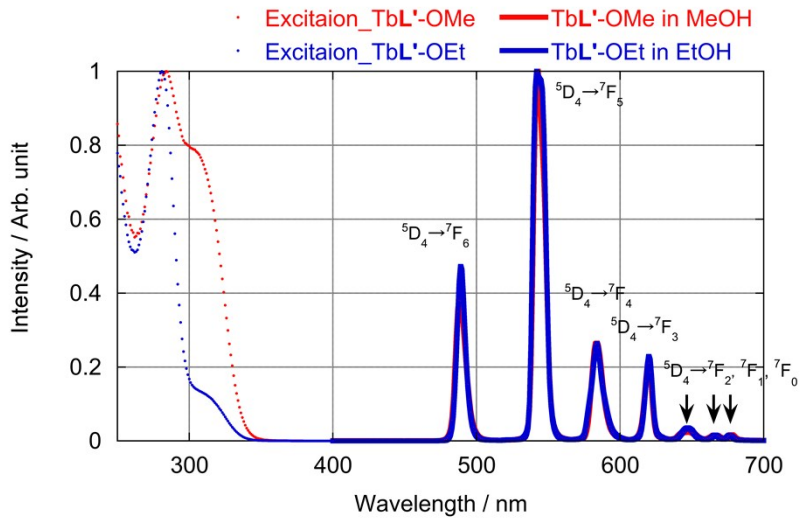

Fig. S8 Normalized luminescence spectra of Tb**L'**-O***R*** complexes (***R*** = Me (red line) in MeOH, ***R*** = Et (blue line) in EtOH) at 298 K and excited at 370 nm (1.0×10^{-4} M). Excitation spectra were recorded by monitoring the emission wavelength at 543 nm.

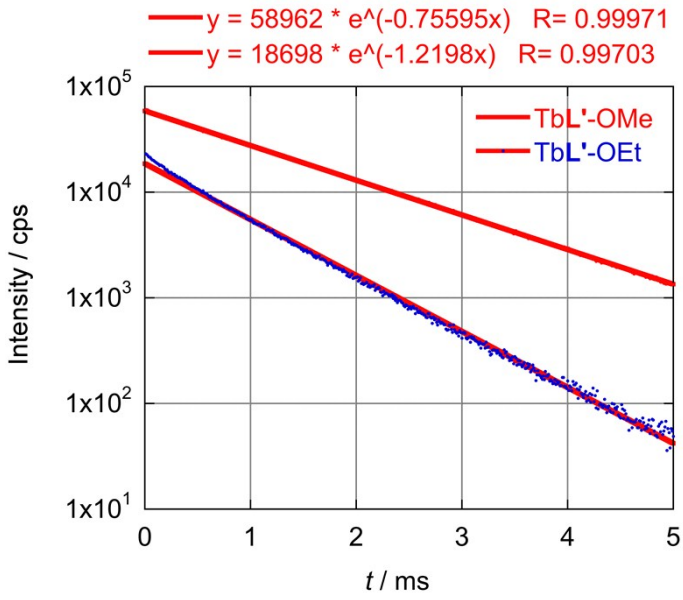

Fig. S9 Luminescence decay curves for Tb**L'**-O***R*** complexes (***R*** = Me (red line), ***R*** = Et (blue line)) in the solid state at 298 K and excited at 370 nm. Data were fitted by a single exponential decay with lifetimes of 1.32 ms and 820 μs for Tb**L'**-OMe and Tb**L'**-OEt, respectively.

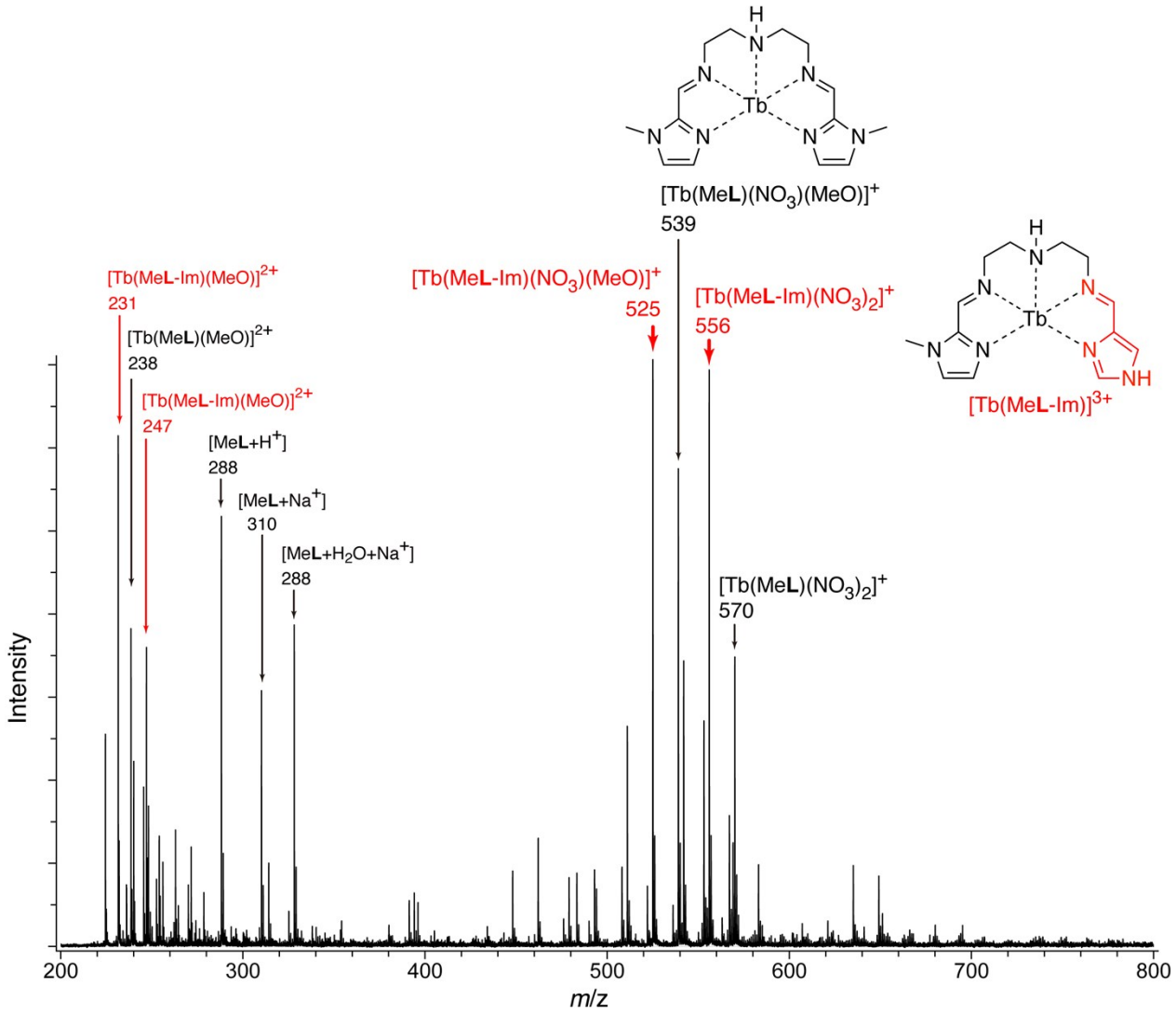

Fig. S10 CSI-MS of reaction mixture (1.0×10^{-4} M) of TbMe**L** and 4-imidazole carbaldehyde (1 equiv.) in MeOH.

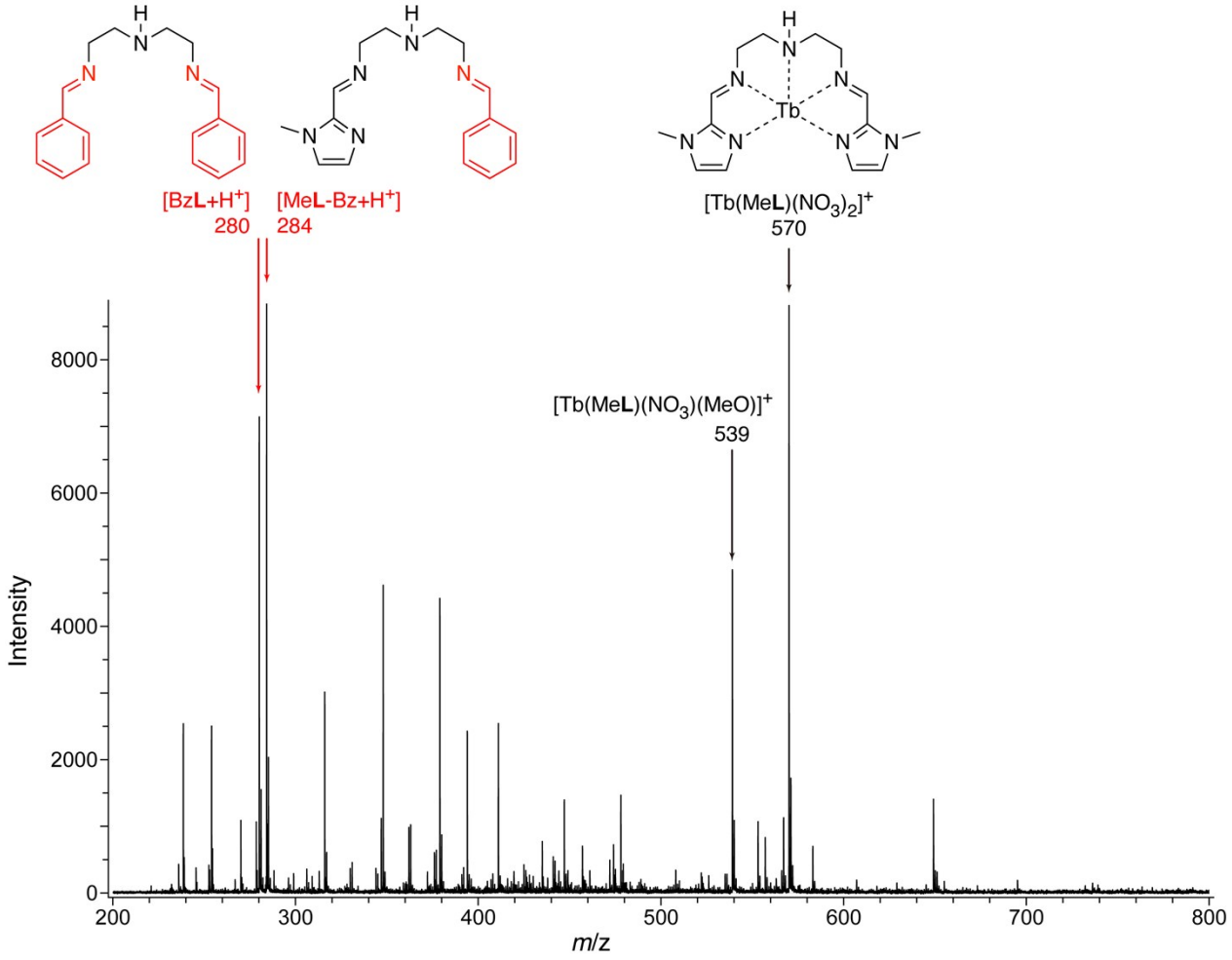

Fig. S11 CSI-MS of reaction mixture (1.0×10^{-4} M) of TbMe**L** and benzaldehyde (1 equiv.) in MeOH.

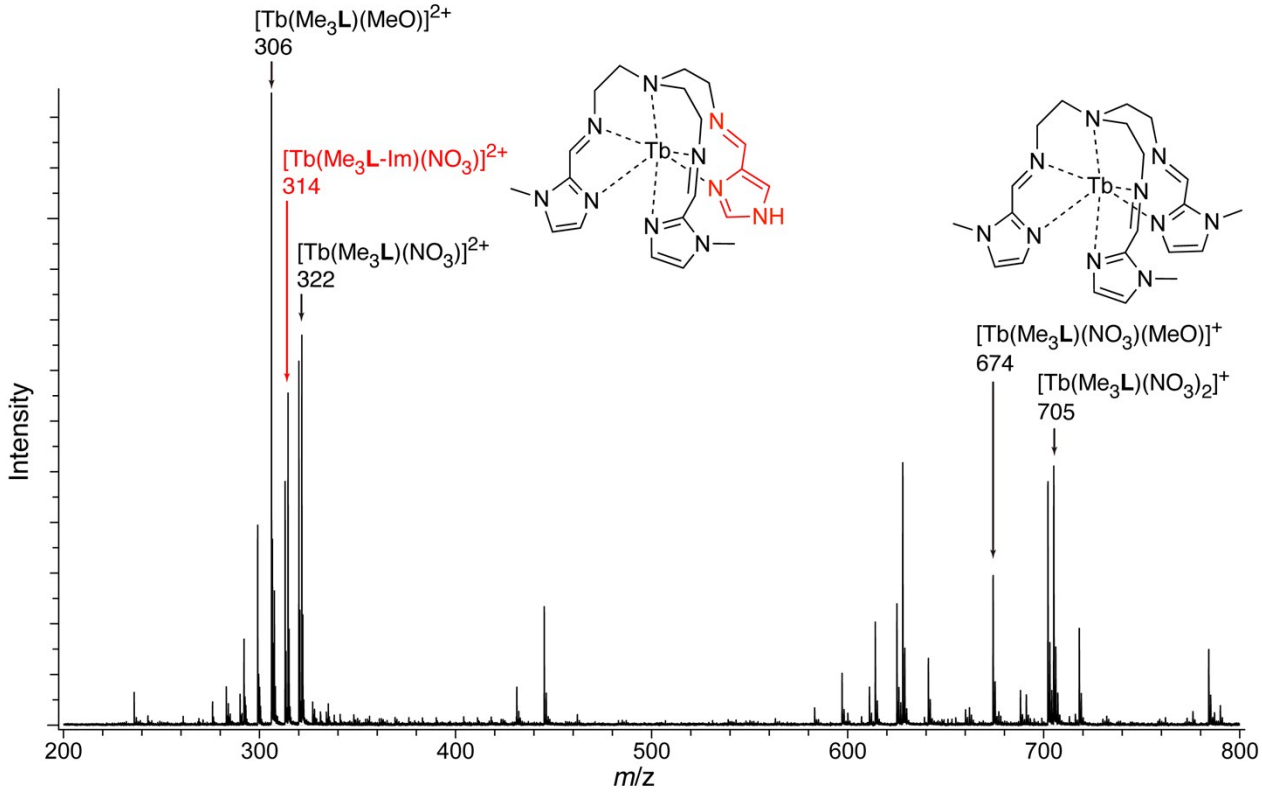

Fig. S12 CSI-MS of reaction mixture (1.0×10^{-4} M) of $TbMe_3$**L** and 4-imidazole carbaldehyde (1 equiv.) in MeOH.

Table S1 Selected bond distances (Å) and angles (°) of ***Ln*L'-O*R*** and ***Ln*HL** (***Ln*** = Tb and Gd).

	Tb**L'**-OMe	Tb**L'**-OEt	Gd**L'**-OMe	Gd**L'**-OEt		TbH**L**	GdH**L**
Distance / Å							
Ln(1)–N(1)	2.899(2)	2.933(6)	2.884(3)	2.945(5)	***Ln***(1)–N(4)	2.653(3)	2.677(4)
Ln(1)–N(2)	2.519(2)	2.523(6)	2.528(3)	2.550(5)	***Ln***(1)–N(5)	2.549(4)	2.569(4)
Ln(1)–N(3)	2.482(2)	2.515(7)	2.501(3)	2.537(5)	***Ln***(1)–N(6)	2.498(3)	2.522(4)
Ln(1)–N(5)	2.499(2)	2.524(7)	2.516(3)	2.540(4)	***Ln***(1)–N(3)	2.490(4)	2.507(4)
Ln(1)–N(6)	2.538(2)	2.518(6)	2.550(3)	2.532(5)	***Ln***(1)–N(2)	2.552(3)	2.575(4)
Ln(1)–N(8)	2.494(2)	2.509(6)	2.517(3)	2.529(4)			
Ln(1)–O(2)	2.536(2)	2.621(6)	2.537(2)	2.609(4)	***Ln***(1)–O(5)	2.534(3)	2.532(3)
Ln(1)–O(3)	2.466(2)	2.484(6)	2.489(2)	2.497(4)	***Ln***(1)–O(6)	2.663(3)	2.672(4)
Ln(1)–O(5)	2.444(2)	2.500(5)	2.463(2)	2.507(4)	***Ln***(1)–O(2)	2.454(3)	2.481(4)
Ln(1)–O(6)	2.609(2)	2.511(5)	2.608(2)	2.524(4)	***Ln***(1)–O(3)	2.580(3)	2.591(3)
Angle / °							
N(1)-***Ln***(1)-N(2)	64.03(6)	60.8(2)	64.23(8)	60.5(1)	N(4)-***Ln***(1)-N(5)	63.3(1)	63.1(1)
N(1)-***Ln***(1)-N(5)	61.64(7)	62.3(2)	61.63(9)	62.8(1)	N(4)-***Ln***(1)-N(3)	63.9(1)	63.5(1)
N(1)-***Ln***(1)-N(8)	62.37(6)	62.4(2)	62.50(8)	62.0(1)			
N(1)-***Ln***(1)-O(3)	117.83(6)	120.2(2)	117.89(7)	119.1(1)	N(4)-***Ln***(1)-O(5)	115.1(1)	116.1(1)
N(1)-***Ln***(1)-O(5)	67.57(6)	71.2(2)	67.52(7)	71.3(1)	N(4)-***Ln***(1)-O(3)	64.3(1)	63.9(1)
N(2)-***Ln***(1)-N(5)	83.10(7)	84.2(2)	82.96(8)	82.4(1)	N(3)-***Ln***(1)-N(5)	124.4(1)	124.1(1)
N(3)-***Ln***(1)-N(6)	73.49(7)	75.0(2)	73.20(9)	74.0(1)	N(2)-***Ln***(1)-N(6)	87.9(1)	89.1(1)
C(1)-N(1)-C(7)	110.4(2)	110.6(6)	110.5(2)	109.9(4)	C(6)-N(4)-C(7)	112.5(4)	112.9(4)

Table S2 Crystallographic data for ***Ln*L'-O*R*** complexes.

	Tb**L'**-OMe	Tb**L'**-OEt	Gd**L'**-OMe	Gd**L'**-OEt
Empirical formula	$C_{18}H_{27}N_{12}O_{11}Tb$	$C_{20}H_{33}N_{12}O_{12}Tb$	$C_{18}H_{27}GdN_{12}O_{11}$	$C_{20}H_{31}GdN_{12}O_{11}$
Fw / g·mol^{-1}	746.43	792.50	744.76	772.82
Temperature / *K*	100	100	100	100
Space group	$P\bar{1}$	$P\bar{1}$	$P\bar{1}$	$P\bar{1}$
a / Å	8.5547(5)	8.705(1)	8.531(1)	8.808(1)
b / Å	11.6314(6)	11.759(2)	11.651(2)	11.790(2)
c / Å	14.5948(8)	16.381(4)	14.664(2)	16.345(2)
α / °	109.526(1)	105.565(3)	109.625(2)	70.900(2)
β / °	94.341(1)	94.096(3)	94.477(2)	87.672(2)
γ / °	100.026(1)	111.197(2)	100.200(2)	68.502(2)
V / Å^3	1333.7(1)	1479.2(5)	1336.2(3)	1486.3(3)
Z	2	2	2	2
D_{calc} / g·cm^{-3}	1.859	1.779	1.851	1.727
Reflections collected	9959	10188	9971	8485
Independent reflections (R_{int})	7410 (0.0166)	7889 (0.0253)	7426 (0.0217)	6003 (0.0147)
No. of variables	389	402	389	399
GOF	1.035	1.167	1.032	1.173
R_1[a] ($I > 2\sigma$)	0.0260	0.0672	0.0333	0.0443
wR_2[b] (all data)	0.0601	0.1513	0.0717	0.1046
CCDC	1557990	1557991	1557996	1557997

[a] $R_1 = \Sigma||F_o| - |F_c||/\Sigma|F_o|$. [b] $wR_2 = [\Sigma w(F_o^2 - F_c^2)^2/\Sigma w(F_o^2)^2]^{1/2}$